

The Use of Multi-Walled Carbon Nanotubes and Titanium Oxide Nano Particles in the Construction of Calcium Ionophore IV Based Calcium-Selective Electrodes

H. Elif Kormalı Ertürün

Department of Chemistry, Faculty of Science, Ankara University, Tandoğan 06100, Ankara, TURKEY
E-mail: kormali@science.ankara.edu.tr

Received: 11 June 2018 / Accepted: 8 August 2018 / Published: 1 September 2018

Calcium ionophore IV (ETH 5234) cocktail (CaIC), multi-walled carbon nanotubes (MWCNTs) and titanium(IV) oxide nanoparticles (TiO₂NPs) were used to fabricate a new highly sensitive and selective modified glassy carbon electrode (CaIC-MWCNT-TiO₂NP /GCE) for the determination of calcium. The surface of the electrode was characterized by scanning electron microscopy (SEM). The effect of various experimental parameters such as membrane composition, construction technics, pH on the potentiometric response of the electrode was investigated. The proposed electrode has a linear response in the $1.0 \times 10^{-7} - 1.0 \times 10^{-1}$ M concentration range, with a near-Nernstian slope (28.5 ± 0.9 mV / pCa), and a low detection limit of 6.9×10^{-8} M. This electrode was used to the determine calcium content of milk, water and pharmaceutical samples and the results were found to be in good agreement with those obtained by atomic absorption spectrophotometry (AAS).

Keywords: Calcium-selective electrode; ETH 5234 (calcium ionophore IV); Calcium determination; Multi-walled carbon nanotubes; Metal oxide nanoparticles

1. INTRODUCTION

Calcium is an element that is essential for living organisms, including humans. It is the most abundant mineral in the body and vital for good health. Bone health, muscle contraction, blood clotting, neuronal activity and many enzymatic reactions in the body are the main responsibilities of calcium. For our health, we need to consume calcium in certain amounts every day [1,2]. It is found naturally in water and much food such as milk and dairy products, meat, vegetables, fruits and nuts. It is also added to certain products which are available as calcium-containing medicines and supplements. Hence, in-vivo and in-vitro determination of calcium is an important task.

Potentiometric measurement of ionized calcium in water, medicine, food and biological fluids [3] has begun to be preferred to other common instrumental methods [4-6] used for this purpose since the first calcium-selective electrode developed by Ross [7]. Low cost, ease of use and excellent selectivity properties are the reason for ion-selective electrodes (ISEs) to be preferred [8-11].

In recent years, the design of solid-contact ISEs with shorter response times, easier miniaturization, availability for in-situ analysis has become more widespread when compared with ISEs containing inner filling solution. They can generally be constructed with a polymer ion-selective membrane, incorporated with plasticizer, ionophore, and nanomaterials coated onto a solid surface. Recently, there have been many studies carried out with nanomaterials since they possess some unique chemical, physical and electronic properties [12,13]. Especially, they are widely applied in the development of new modified ISEs.

Carbon nanotubes with enhanced physical properties such as mechanical [14], electrical [15] and thermal [16] have generated a promising research area since their invention [17,18]. Most significantly, much research has interested in nanotubes for mechanical reinforcement of polymers [19,20]. Besides them, metal nanoparticles are also employed for sensor development to improve its performance. Their large surface area and high ratio of surface to bulk atoms ensure enhanced catalytic activity compared with corresponding bulk metals [21,22].

The main component responsible for the selectivity of the ISEs is ionophore. There are a large number of neutral or charged ionophores used in the preparation of calcium-selective electrodes in the literature [23-37]. Like the calcium ionophore IV (ETH 5234) cocktail used in this study, ready-to-use membrane cocktails of some of these ionophores are commercially available.

In this study; it was aimed to construct an ETH 5234 (Fig. 1) based solid-contact Ca^{2+} -selective electrode with a wide working range, Nernstian slope, high selectivity, stable, short response time and high reproducibility by combining the advantages of solid-contact membrane electrodes, multi-walled carbon nanotubes (MWCNTs) and metal oxide nanoparticles (MONPs) together which then can be applied to a wide range of samples.

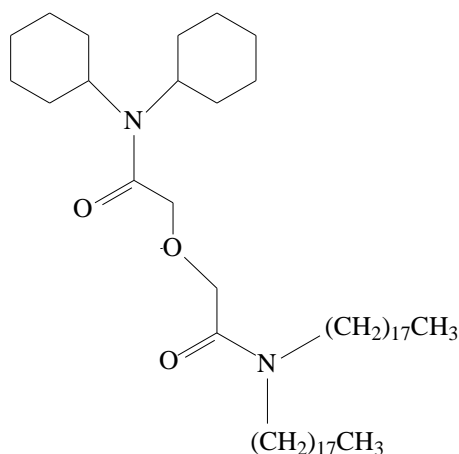


Figure 1. Structure of N,N-dicyclohexyl-N',N'-dioctadecyl-3-oxapentanediamide (Calcium ionophore IV: ETH 5234).

2. EXPERIMENTAL

2.1. Chemicals and solutions

Calcium ionophore IV cocktail containing ETH 5234 (0.072 wt. %), *o*-nitrophenyl octyl ether (*o*-NPOE) (4.748 wt. %), poly (vinyl chloride) (PVC) (2.379 wt. %), potassium tetrakis (4-chlorophenyl) borate (KTPCIPB) (0.022 wt. %), and tetrahydrofuran (THF) (92.780 wt. %) was selectophore reagent purchased from Fluka (solution 1).

MWCNTs (outer diameter < 8 nm, length 10–30 μm , and purity >95%) were obtained from Cheaptubes Inc. (Brambleboro, USA) and dispersion of 0.5 mg of MWCNTs in 1 mL of THF (solution 2) was used for coating.

Titanium oxide nanoparticles (TiO_2NPs) (<150 nm) and other MONPs were bought from Sigma (St. Louis, MO, USA). 1.0 mg of MONPs was dispersed in 1 mL of THF (solution 3).

All other chemicals were of analytical-reagent grade provided from Merck, Sigma-Aldrich or Riedel-de Haën.

2.2. Fabrication of the coated electrodes

Glassy carbon electrodes (GCE) were polished with alumina suspension on an alumina polishing pad. After rinsing several times with water, finally sonicated in ethanol and deionized water for 15 min, successively before each coating.

The electrodes were prepared by coating in two different ways:

(i) Type 1: The portions taken in equal volumes from solutions 1, 2 and 3 were thoroughly mixed with the vortex, and 10 μL of this mixture was dropped onto the GCE surface (CaIC-MWCNT- TiO_2NP /GCE), then left to dry.

(ii) Type 2: Unlike the method in Type 1, before coating GCE surface with 5 μL of solution 1, 5 μL of the mixture prepared by mixing equal volumes of solution 2 and 3 was dropped onto the GCE surface and dried in room temperature (CaIC/MWCNT- TiO_2NP /GCE).

2.3. Instruments and measurements

Double-distilled water supplied from ELGA Purelab Classic Ultrapure Water System (High Wycombe, Bucks, UK) was used for the preparation of all aqueous solutions.

All potentials were measured with a 16-channel data system (Lawson Labs Inc., Malvern, PA, USA) using a double-junction Ag/AgCl electrode (Orion 900200) as the reference electrode.

The surface morphologies of the electrodes were examined by scanning electron microscopy (SEM.: FEI Quanta 450 FEG, Hillsboro, USA).

Impedance measurements of electrodes were carried out with CHI660D Electrochemical Workstation (Austin, TX, USA) at ambient temperature. Modified GCEs, platinum wire, and Ag/AgCl

electrode were used as the working electrodes, the counter electrode, and the reference electrode, respectively.

The GBC Avanta atomic absorption spectrophotometer (AAS) (Melbourne, Australia) was used to determine calcium content of real samples for comparison of results obtained with the proposed electrode.

2.4. Real samples

Effervescent tablets and antacid chewable tablets (Basel and GlaxoSmithKline products, respectively), used as pharmaceutical samples, containing 1000 mg of calcium per tablet, were purchased from local pharmacy in Ankara, Turkey. Long life cow milk and mineral water were supplied from local markets in Ankara, Turkey. Ankara's tap water was used as a water sample.

To prepare the solutions of tablets, initially the drug content of ten tablets was weighed and powdered in a porcelain mortar. The average mass per tablet was determined. A sample equivalent to five tablets was weighed and boiled with 15 mL HNO₃ and 3 mL H₂O₂ for at least half an hour for the dissolution of calcium, and transferred into the volumetric flask of 1000.0 mL and diluted to the mark with deionized water. The contents of the flask were sonicated for 30 min to achieve complete dissolution. A 25 mL aliquot from the milk sample was prepared by boiling with 15 mL HNO₃ and 3 mL H₂O₂ in the same manner. Total volume of this solution was 250 mL. The prepared tablets and milk samples were allowed to rest in the refrigerator for at least 12 hours so that the undissolved portions could be completely precipitated. Clear supernatant liquids from these samples were used for determination of calcium. Samples of mineral water and tap water were diluted, 1:5 and 1:2, respectively.

Appropriate quantities from the above mentioned stock sample solutions were transferred to 50 mL flasks containing 5 mL of 1 M sodium chloride and 5 mL of acetic acid / sodium acetate buffer, and the volume was adjusted to 50 mL with deionized water. The determination of calcium was performed in real samples by using direct calibration method.

3. RESULTS AND DISCUSSION

3.1. Membrane optimization

Due to the chemical stability, excellent electrical conductivity and electrocatalytic activity properties of high-performance materials such as carbon nanotubes and inorganic nanoparticles, embedding them in polymer matrices, results in highly selective and sensitive materials for the fabrication of electrodes which can be used in broad range of research areas [20,21].

For this reason, the effect of MWCNT content and the MONP type on the performance of the solid-contact Ca²⁺-selective electrode based on ETH 5234 was investigated in this study. For this purpose, in order to optimize the MWCNT content on the electrode surface, three electrodes were prepared (E2, E3 and E4) by changing its amount as 0.25, 0.50 and 1.00 µg in the preliminary experiments. To examine the effect of MWCNT, an electrode (E1) free of MWCNT was also prepared.

The response characteristics obtained for electrodes E1-E4 are given in Table 1. As it is obvious, no significant contribution to electrode performance was observed in terms of working range, slope and detection limit. The optimal amount of MWCNT on the electrode surface was taken as 0.25 μg since the slope and limit of detection (LOD) of E2 were relatively better than the other electrodes and incorporation of MWCNT generally showed decreased electrode resistances [20].

To investigate the effect of MONP type on the electrode performance six different electrodes (E5-E10) were prepared by adding metal oxide nanoparticles such as TiO_2 , ZnO, CuO, Fe_2O_3 , Co_3O_4 and SnO_2 to the Ca^{2+} -selective membrane cocktail without MWCNT to have a fixed amount of each 0.50 μg on the surface of the electrodes. There was no significant improvement in the performance of electrodes prepared with different MONPs with regard to the slopes and working ranges when compared with that of MONP-free electrode (E1). Furthermore, the electrode with Co_3O_4 (E9) exhibited the narrowest working range while the one with Fe_2O_3 (E8) demonstrated the lowest slope. Moreover, Ca^{2+} -selective electrode (E11) was prepared by incorporation of 0.25 μg MWCNT and 0.50 μg TiO_2 in addition to Ca^{2+} ionophore in the membrane in order to evaluate whether the use of these materials together can affect the performance of the electrode or not. As shown in the Table 1, the slope of this electrode was found to be almost Nernstian as well as the other electrodes, while its working range was found to be wider and its LOD was lower than the rest of the electrodes. The improvement can be attributed to the synergistic effect of MWCNTs and TiO_2 NPs on the performance of the electrode.

Additionally, the effect of coating way was investigated by comparing the response behavior of the electrode E11 with that of E12 which were constructed according to coating way Type 1 and Type 2, respectively as indicated in the experimental section. It was concluded that the coating way Type 1 was more suitable when the performance of E11 and E12 were compared. Although there was no significant difference between their performance characteristics, coating way Type 1 for the fabrication of solid-contact electrode has an advantage of ease of preparation in a short time by dropping appropriate amount of the mixture containing all components at once.

Table 1. Optimization of MWCNT amount and kind of MONPs in calcium-selective membranes of CaIC-MWCNT -MONP/GCE

Electrode	MWCNTs (μg)	MONPs (0.50 μg)	Slope \pm t_s/\sqrt{N} (mV/pCa) ^a	Linear range (M)	LOD (M)
1	-	-	26.0 \pm 1.4	$1.0 \times 10^{-6} - 1.0 \times 10^{-1}$	6.1×10^{-7}
2	0.25	-	27.3 \pm 1.4	$1.0 \times 10^{-6} - 1.0 \times 10^{-1}$	2.7×10^{-7}
3	0.50	-	25.0 \pm 2.1	$1.0 \times 10^{-6} - 1.0 \times 10^{-1}$	9.5×10^{-7}
4	1.00	-	21.3 \pm 2.9	$1.0 \times 10^{-6} - 1.0 \times 10^{-1}$	4.2×10^{-7}
5	-	TiO_2	28.4 \pm 1.5	$1.0 \times 10^{-6} - 1.0 \times 10^{-1}$	4.9×10^{-7}
6	-	ZnO	27.2 \pm 1.3	$1.0 \times 10^{-6} - 1.0 \times 10^{-1}$	3.9×10^{-7}
7	-	CuO	27.6 \pm 1.8	$1.0 \times 10^{-6} - 1.0 \times 10^{-1}$	7.0×10^{-7}
8	-	Fe_2O_3	24.7 \pm 1.8	$1.0 \times 10^{-6} - 1.0 \times 10^{-1}$	5.0×10^{-7}
9	-	Co_3O_4	27.4 \pm 1.9	$1.0 \times 10^{-5} - 1.0 \times 10^{-1}$	5.3×10^{-6}
10	-	SnO_2	26.9 \pm 1.3	$1.0 \times 10^{-6} - 1.0 \times 10^{-1}$	4.9×10^{-7}
11	0.25	TiO_2	28.5\pm0.9	$1.0 \times 10^{-7} - 1.0 \times 10^{-1}$	6.9×10^{-8}
12 ^b	0.25	TiO_2	30.8 \pm 1.3	$1.0 \times 10^{-7} - 1.0 \times 10^{-1}$	8.5×10^{-8}

^a $N=5$; ^b Type 2

3.2. Surface Characterization

SEM was used to examine the change of membrane morphology after the addition of MWCNTs and MONPs to the membrane cocktail separately (Fig. 2b, 2c), and simultaneously (Fig. 2d). For this purpose, three different electrodes called as CaIC-MWCNT/GCE, CaIC-TiO₂NP/GCE and CaIC-MWCNT-TiO₂NP/GCE were prepared. CaIC/GCE (Fig. 2a) was also constructed for comparison purposes. SEM images of these electrodes given below showed that Ca²⁺-selective cocktail components were homogeneously distributed as agglomerates in the membrane (Fig. 2a). The resulting membrane obtained after the incorporation of MWCNTs and TiO₂NPs to this membrane cocktail were found to have smooth sections (Fig. 2b) and bright spotty regions on agglomerates (Fig. 2c), respectively. The bright spotty regions appeared in Fig. 2c may belong to TiO₂NPs. Finally, it was thought that the components were homogeneously distributed in the membrane shown in Fig. 2d due to the observation of all characteristics seen in Fig. 2a, 2b and 2c.

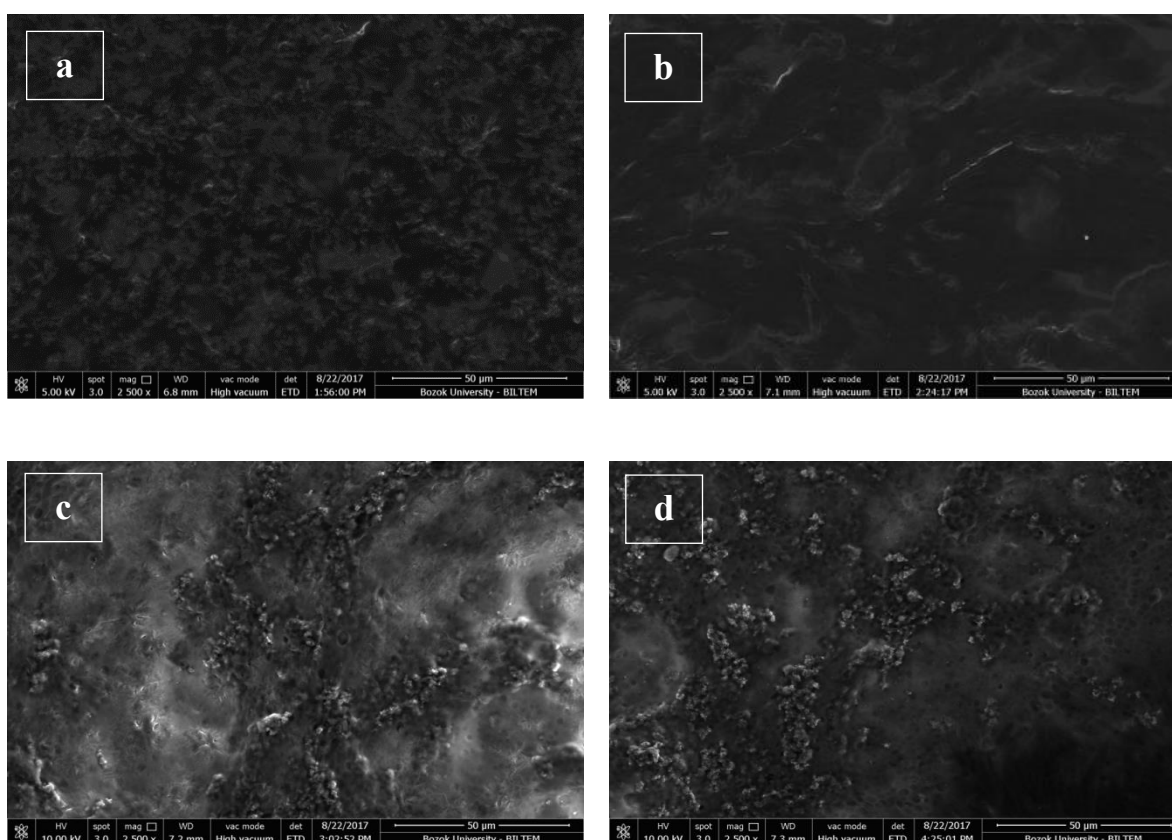


Figure 2. The SEM images of (a) CaIC/GCE, (b) CaIC-MWCNT/GCE, (c) CaIC-TiO₂NP/GCE and (d) CaIC-MWCNT-TiO₂NP/GCE.

3.3. The impedance measurements

The electrochemical impedance spectroscopy (EIS) method is an effective method for studying the effect of membrane components and electrode preparation techniques on the membrane resistance due to their capability of changing the properties of the modified electrodes and the interface [38].

Plotting the Nyquist curves of the electrodes (a) CaIC/GCE, (b) CaIC-MWCNT/GCE, (c) CaIC-TiO₂NP/GCE and (d) CaIC-MWCNT -TiO₂NP/GCE in the acetic acid / acetate buffer was aimed to interpret the effect of each component in the electrode membranes (Fig. 3A).

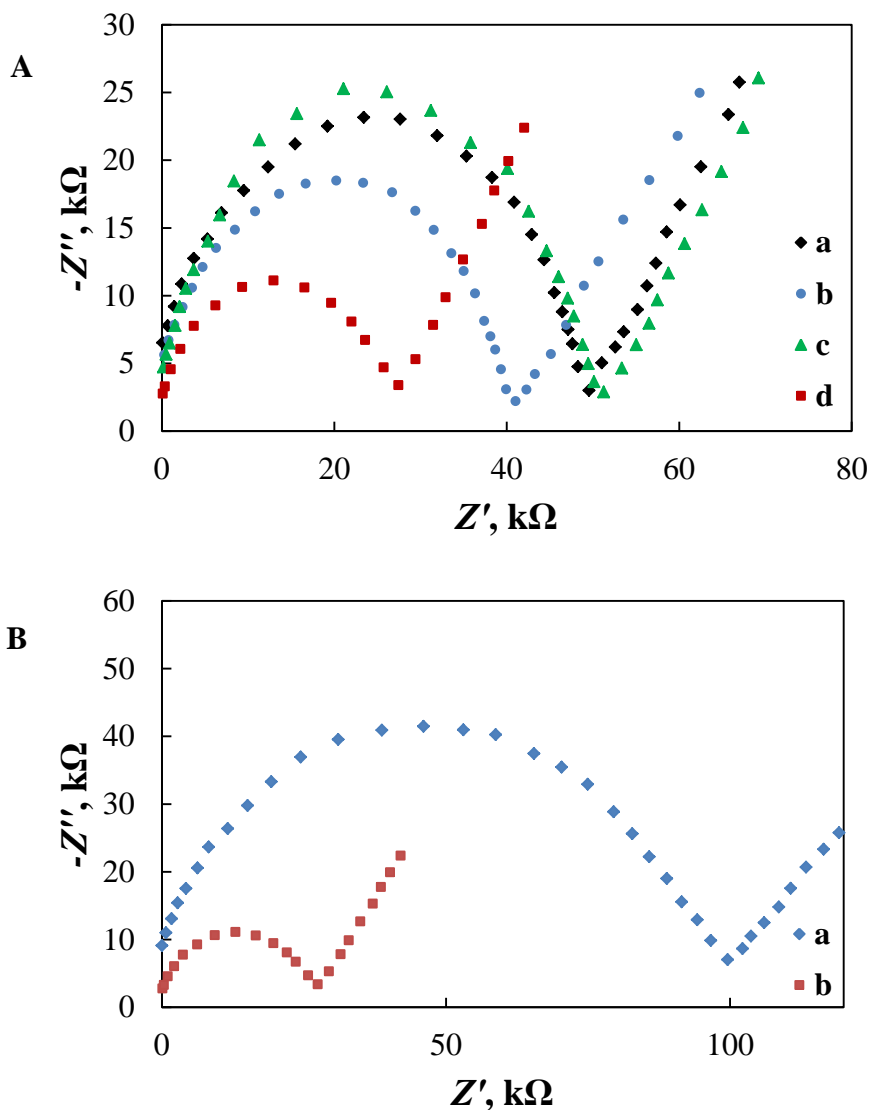


Figure 3. Nyquist plots of **A:** (a) CaIC/GCE, (b) CaIC-MWCNT/GCE, (c) CaIC-TiO₂NP/GCE and (d) CaIC-MWCNT -TiO₂NP/GCE and **B:** (a) CaIC/MWCNT-TiO₂NP/GCE (type2) and. (b) CaIC-MWCNT-TiO₂NP/GCE (type 1) in acetic acid/acetate buffer solution (pH 4) containing 1.0×10^{-3} M CaCl₂ and 0.1 M NaCl.

Each of these curves consists of a semi-circular part showing the electron transfer resistance (R_{ct}) at low frequencies and a linear section supporting the response of the electrode depending on the diffusion of Ca²⁺ ion at high frequencies. Although the TiO₂NPs are used as semiconductors, it was seen that the membrane resistance of curve (c) slightly increased with the introduction of TiO₂NPs to the CaIC/GCE membrane (curve a). However, the membrane resistance was significantly decreased when MWCNT (curve b) and MWCNT + TiO₂NP (curve d) were added to the same CaIC/GCE

membrane. The improvement in conductivity of these membranes containing MWCNT can be attributed to the high electrical conductivity of MWCNTs. Further reduction of membrane resistance for the electrode prepared with MWCNT + TiO₂NP (curve d) could be due to a more homogeneous distribution of TiO₂NP together with MWCNT in the membrane without aggregation when compared with the membrane of CaIC-TiO₂NP/GCE (curve c). In addition, the question whether the coating way Type 1 and Type 2 affect the membrane resistance or not was studied. For this purpose, Nyquist curves of the electrodes with same membrane components prepared by Type 1 (CaIC-MWCNT-TiO₂NP /GCE) and Type 2 (CaIC/MWCNT-TiO₂NP/GCE) were drawn and given in Fig. 3B. CaIC-MWCNT-TiO₂NP /GCE's (type 1, curve b) membrane showed much lower resistance than the electrode fabricated by coating way Type 2 (curve a). This situation could be the result of decreased conductivity or increased membrane resistance due to the use of coating way Type 2, in which the conductive MWCNT+TiO₂NP/GCE surface was finally insulated by being coated with plasticized PVC containing CaIC cocktail.

On the basis of the membrane optimization and impedance studies, the performance characteristics of the Ca²⁺-selective solid-contact electrode were determined with E11 prepared according to coating way Type 1.

3.4. Performance Characteristics

The optimum pH for the electrode was determined prior to examine its performance characteristics of the electrode. For this purpose, potential values were measured in two series of calibration solutions prepared by changing the pH in the range of 2-12 adjusted with additions of HCl and NaOH solutions. These series contained 0.1 M NaCl as an ionic strength adjuster and 1.0×10^{-2} or 1.0×10^{-3} M Ca²⁺. Electrode response was found to be stable in the range pH 3-5. Therefore, pH 4 was selected as the working pH to perform all measurements in this study.

The linear working range, the slope and the LOD of E11 (CaIC-MWCNT-TiO₂NP/GCE) prepared with the optimum membrane composition were determined by using chronopotentiometric data. Potential-time (*E-t*) graph of the electrode for step changes in calcium concentrations containing buffer solution together with ionic strength adjuster was given in Fig. 4A. The potential values found by the help of the *E-t* graphs were plotted against the pCa values, and the calibration graphs were obtained with the error bars for five replicates (Fig. 4B). The working range, slope and LOD of the electrode were found to be 1.0×10^{-7} - 1.0×10^{-1} M, 28.5 ± 0.9 .mV / pCa and 6.9×10^{-8} M, respectively. This indicated that the solid-contact potentiometric electrode had a Nernstian behavior in a wide working range and demonstrated competing performance characteristics with many Ca²⁺-selective electrodes given in the literature.

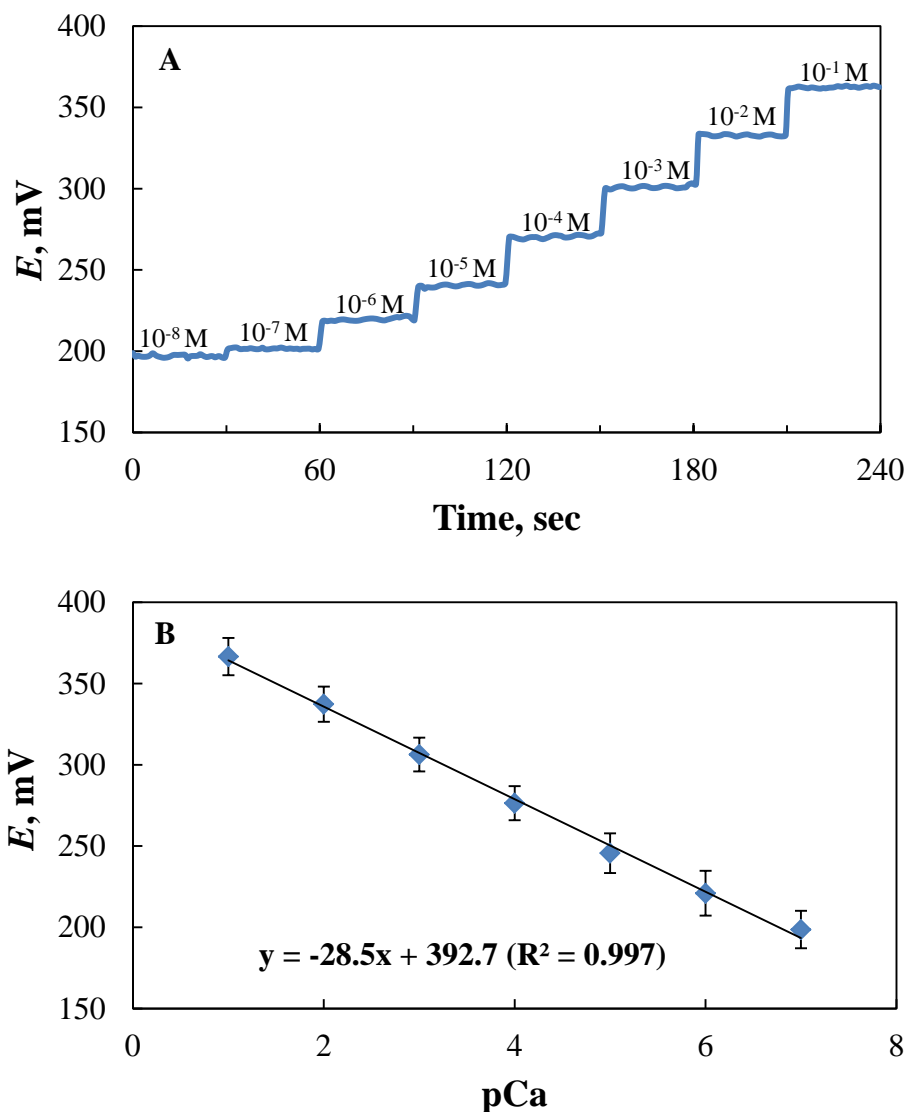


Figure 4. (A) Chronopotentiometric response and (B) typical calibration graph ($N= 5$) of CaIC-MWCNT-TiO₂NP/GCE plotted with error bars by the data obtained for step changes in calcium concentration in solutions containing 0.1 M acetic acid/acetate (pH = 4.0) and 0.1 M NaCl.

Potentiometric selectivity coefficients of Ca²⁺-selective solid-contact electrode were determined for various cations using fixed interference method (FIM) by plotting the calibration curves for Ca²⁺ in the presence of interfering ions kept at a constant concentration of 10⁻² M. From the calibration curves, the intersection of two linear portions was used to determine the lowest Ca²⁺ concentration to be used in the formulation to calculate the selectivity coefficients. The data obtained were given in Table 3. It was observed that many cations had very negligible effect on the potentiometric response of the electrode. However, it can be said that Sr²⁺, Pb²⁺, Ag⁺, Cs⁺, K⁺, Li⁺ and Na⁺ can partially act on the electrode response at high concentrations. As a result, in the presence of these cations calcium content in many real samples can be determined satisfactorily.

Table 2. Comparing some of electrode characteristics of CaIC-MWCNT-TiO₂NP/GCE with previous Ca²⁺ - selective electrodes based on ETH 5234 ionophore

Ref.	ISM*/Electrode type	Slope (mV/pCa)	Linear range (M)	LOD (M)	Response time (s)
30	⁽ⁱ⁾ ISM/Fe ₃ O ₄ -rGO/Au	28.2 ±0.7	1.0×10 ⁻⁶ -1.0×10 ⁻³	4.0×10 ⁻⁷	10-20
31	⁽ⁱⁱ⁾ ISM/PPy (pTS)/PVDF	27.7	1.0×10 ⁻⁶ -1.0×10 ⁻³		
32	⁽ⁱⁱⁱ⁾ ISM/Conductive Mat./Cu	25±6	1.0×10 ⁻⁵ -1.0×10 ⁻¹	1×10 ⁻⁶	<10
33	^(iv) ISM/ZnSe/GCE	25.5±1.2	1.0×10 ⁻⁷ -2×10 ⁻⁵	2×10 ⁻⁸	
	^(v) ISM/ZnSe/POT/GCE	27.3±0.1	1.0×10 ⁻⁸ -1.0×10 ⁻⁴	8×10 ⁻⁹	
34	^(vi) ISM/PDOT/GCE	24.1±0.5	1.0×10 ⁻¹⁰ -1.0×10 ⁻²		20
35	^(vii) ISM/PEDOT(PSS)/Au	~30	1.0×10 ⁻⁶ -1.0×10 ⁻²	2×10 ⁻⁷	
	^(viii) ISM/PEDOT(TFPB)/Au	~30	1.0×10 ⁻⁶ -1.0×10 ⁻³	2×10 ⁻⁷	
36	^(ix) ISM/PPyCl/GCE	26.7±0.6	1.0×10 ⁻⁴ -1.0×10 ⁻¹	~10 ⁻⁵	
37	^(x) PEDOT/PSS/ISM/PE	27.9±0.9	1.0×10 ⁻⁸ -1.0×10 ⁻¹	5×10 ⁻⁹	
This work	^(xi) ISM/GCE	28.5±0.9	1.0×10 ⁻⁷ -1.0×10 ⁻¹	6.9×10 ⁻⁸	4-5

*ISM: Ion-selective membrane: ⁽ⁱ⁾ *o*-NPOE, sodium tetrakis[3,5-bis(trifluoromethyl) phenyl] borate (NaTFPB), PVC; ⁽ⁱⁱ⁾ *o*-NPOE, sodium tetrakis (4-chlorophenyl) borate (NaTCIPB), PVC; ⁽ⁱⁱⁱ⁾ ETH 500, KTpCIPB; ^(iv and v) dioctyl sebacate (DOS), potassium tetrakis[3,5-bis (trifluoromethyl)phenyl] borate (KTFPB), PVC; ^(vi) 1,6-hexanedioldiacrylate, 2,2-dimethoxy-2-diphenyl acetophenone, *n*-butyl acrylate, sodium and calcium salts of tetrakis[3,5 bis(trifluoromethyl) phenyl] borate anions; ^(vii and viii) *o*-NPOE, KTFPB; ^(ix) *o*-NPOE, NaTFPB, PVC; ^(x) DOS, NaTFPB, PVC; ^(xi) CaIC, MWCNTs, TiO₂NPs containing ETH 5234 as an ionophore.

Table 3. Selectivity coefficients of CaIC-MWCNT-TiO₂NP/GCE determined by FIM

Interfering ions	Selectivity coefficient (log K ^{pot} _{A,B})	Interfering ions	Selectivity coefficient (log K ^{pot} _{A,B})
Ba ²⁺	-2.9	Pb ²⁺	-1.7
Sr ²⁺	-1.9	Zn ²⁺	-3.9
Mg ²⁺	-3.2	Fe ³⁺	-4.5
Cd ²⁺	-3.0	Ag ⁺	-1.3
Co ²⁺	-3.5	Cs ⁺	-1.8
Cu ²⁺	-3.6	K ⁺	-1.8
Hg ²⁺	-2.8	Li ⁺	-1.9
Mn ²⁺	-3.4	Na ⁺	-1.9
Ni ²⁺	-3.7	NH ₄ ⁺	-2.5

The stability of the potentiometric response of solid-contact electrodes is related to the presence of a water layer between the ion-selective membrane and the solid substrate. In the presence of a water layer, instable response behavior occurs when the ion-selective electrode is immersed in three different solutions in the sequence of the target ion solution, the interfering ion solution, and target ion solution

again. The deviations, observed when recording the potentials during a specified period of time, are the evidence of instable responses due to the change of ion content in the water layer [30,39].

The proposed CaIC-MWCNT-TiO₂NPs/GCE electrode was first immersed in 10⁻³ M Ca²⁺ solution prepared in 0.1 M acetic acid / acetate (pH = 4.0) buffer containing 0.1 M NaCl and a potential-time graph was plotted (Fig. 5). The other potentials were recorded after immersing the electrode firstly in 10⁻³ M interfering ion solution in given media and secondly the target ion solution again. For this purpose, two different interfering ions, which were found to be the most interfering ones such as Sr²⁺ and K⁺, were used separately in water layer test. As can be seen in Fig. 5, the electrode reached the same equilibrium potential value before and after contact with the interfering ion. This observation indicated that there was no water layer between the solid substrate and the ion-selective membrane.

The main reason for this case can be the presence of hydrophobic MWCNT in the ion-selective membrane that avoids the formation of water layer. Similar results were found for the previously reported solid-contact electrodes containing MWCNT in the literature [40,41]. It can also be said that the absence of water layer in the proposed electrode provided advantages such as repeatable potential measurements and reasonable long life time.

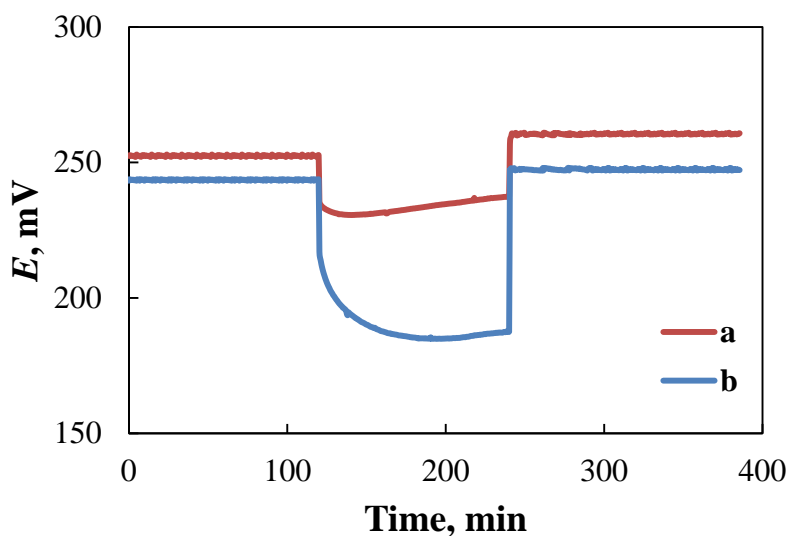


Figure 5. Water layer test for CaIC-MWCNT-TiO₂NP/GCE. Interfering ions: (a) Sr²⁺ and (b) K⁺

3.5. Real Sample Analysis

The applicability of highly selective and stable CaIC-MWCNT-TiO₂NP/GCE in various samples for the determination of calcium was investigated. Five different samples were selected and their Ca contents were determined by direct calibration method. The results were given in Table 4. To test the accuracy of the results, Ca contents of same samples were also determined by using AAS. It was seen that the results obtained with potentiometric method were in good agreement with that of AAS. It can be concluded that CaIC-MWCNT-TiO₂NP/GCE could be successfully employed in

various calcium containing medicines, water samples. This electrode can also be used for quality control purposes in various real samples.

Table 4. Determination of calcium contents in some real samples using atomic absorption spectroscopy and the proposed CaIC-MWCNT-TiO₂NP/GCE

Sample	Potentiometry	AAS	Labeled value
		(mg/tablet)	
Effervescent tablet	1019.5 ± 37.8	1015.1 ± 42.8	1000
Antacid chewable tablet	1005.9 ± 70.8	1046.7 ± 83.8	1000
		(mg L ⁻¹)	
Long life cow milk	1097.6 ± 72.8	1070.4 ± 81.2	1148
Mineral water	234.8 ± 6.4	237.5 ± 5.6	235.5
Tap water	47.9 ± 4.2	45.97 ± 3.8	-

4. CONCLUSIONS

For the first time in this study, MWCNTs and TiO₂NPs were successfully used together to construct Ca²⁺-selective electrode.

Although the same materials were used to prepare electrode membranes, it was observed that there were significant differences in the membrane resistances of these electrodes prepared by changing the coating sequence of the components.

It was determined that the proposed electrode exhibited better and / or competitive performance characteristics than many ETH 5234 based Ca²⁺-selective electrodes available in the literature.

It was also shown that the proposed electrode could be successfully used as an indicator electrode for the potentiometric determination of calcium in many real samples. This sensor with high Ca selectivity can be used for routine analysis, quality control purposes and can be miniaturized for in vivo measurements in the future.

ACKNOWLEDGEMENTS

This study was financially supported by Ankara University Scientific Research Projects Coordination Unit, project no: 10B4240003.

References

1. C. Nordqvist, Calcium: Health benefits, foods, and deficiency, (2017) Medical News Today.
2. G.D. Aurbach, S.J. Marx and A.M. Spiegel, Williams Textbook of Endocrinology, 8th ed., W. B. Saunders Co., (1992) Philadelphia, USA.
3. N. Abramova, J. Moral-Vico, J. Soley, C. Ocaña and A. Bratov, *Anal Chim Acta*, 943 (2016) 5.
4. D. Uždavinienė and S. Tautkus, *Chemija*, 18 (2007) 34.
5. N.J. Miller-Ihli and S.A. Baker, *J Food Compos Anal*, 14 (2001) 619.
6. A. Lopez-Moliner, V.T. Cubero, R.D. Irigoyen and D.S. Piazuolo, *Talanta*, 103 (2013) 236.

7. J.W. Ross, *Science*, 156 (1967) 1378.
8. A. Bratov, N. Abramova and A. Ipatov, *Anal Chim Acta*, 678 (2010) 149.
9. J. Bobacka, A. Ivaska and A. Lewenstam, *Chem Rev*, 108 (2008) 329.
10. H.E. Kormalı Ertürün, *Int. J. Electrochem. Sci.*, 12 (2017) 10737.
11. P. Pan, Z. Miao, L. Yanhua, Z. Linan, R. Haiyan, K. Pan and P. Linpei, *Int. J. Electrochem. Sci.*, 11 (2016) 4779.
12. T.J. Yin and W. Qin, *Trends Anal. Chem.*, 51 (2013) 79.
13. A. Düzgün, G.A. Zelada-Guillén, G.A. Crespo, S. Macho, J. Riu and F.X. Rius, *Anal. Bioanal. Chem.*, 399 (2011) 171.
14. A.B. Dalton, S. Collins, E. Muñoz, J.M. Razal, V.H. Ebron, J.P. Ferraris, J.N. Coleman, B.G. Kim and R.H. Baughman, *Nature*, 423 (2003) 703.
15. J.K.W. Sandler, J.E. Kirk, I.A. Kinloch, M.S.P. Shaffer and A.H. Windle, *Polymer*, 44 (2003) 5893.
16. C. Wei, D. Srivastava and K. Cho, *Nano Lett.*, 2 (2002) 647.
17. S. Iijima, *Nature* 354 (1991) 56.
18. R.H. Baughman, A.A. Zakhidov and W.A. Heer, *Science*, 279 (2002) 787.
19. M. Cadek, J.N. Coleman, K.P. Ryan, V. Nicolosi, G. Bister, A. Fonseca, J.B. Nagy, K. Szostak, F. Béguin and W.J. Blau, *Nano Lett.*, 4 (2004) 353.
20. I.N. Mazov, V.L. Kuznetsov, D.V. Krasnikov, N.A. Rudina, A.I. Romanenko, O.B. Anikeeva, V.I. Suslyayev, E.Y. Korovin and V.A. Zhuravlev, *J. Nanotechnol.*, 2011 (2011) 1.
21. X. Niu, W. Yang, H. Guo, J. Ren, J. Liu and J. Gao, *Can. J. Chem.*, 93 (2015) 648.
22. J.E. Parka, S.G. Park and N. Oyama, *Electrochim. Acta*, 50 (2004) 899.
23. A. Vijayalakshmi and J.T. Selvi, *Chem Sci Trans.*, 2 (2013) 246.
24. L. Kou, M. Fua and R. Liang, *RSC Adv.*, 7 (2017) 43905.
25. K. Sharma and M. Rangi, *Asian J. Research Chem.* 4 (2011) 1269.
26. H. Xu, Y. Wang, Z. Luo and Y. Pan, *Meas. Sci. Technol.*, 24 (2013) 125105.
27. J. Ganesh Ummadi, C.J. Downs, V.S. Joshi, J.L. Ferracane and D. Koley, *Anal. Chem.*, 88 (2016) 3218.
28. I. Bedlechowicz-Śliwakowska, P. Lingenfelter, T. Sokalski, A. Lewenstam and M. Maj-Żurawska, *Anal Bioanal Chem*, 385 (2006) 1477.
29. Y.O. Kondratyeva, E.V. Solovyeva, G.A. Khripoun and K.N. Mikhelson, *Electrochim. Acta*, 259 (2018) 458.
30. T. Yin, X. Jiang and W. Qin, *Anal Chim Acta*, 989 (2017) 15.
31. M. Akieh-Pirkanniemi, G. Lisak, J. Arroyo, J. Bobacka and A. Ivaska, *J Membrane Sci*, 511 (2016) 76.
32. G. Vardar, M. Altıkatoğlu, D. Ortaç, M. Cemek and I. Işıldak, *Biotechnology and Applied Biochemistry*, 62 (2015) 663.
33. T. Lindfors, F. Sundfors, L. Höfler and R.E. Gyurcsányi, *Electroanalysis*, 23 (2011) 2156.
34. A. Michalska, K. Pyrzyńska and K. Maksymiuk, *Anal. Chem.*, 80 (2008) 3921.
35. F. Sundfors, R. Bereczki, J. Bobacka, K. Tóth, A. Ivaska and R.E. Gyurcsányi, *Electroanalysis*, 18 (2006), 1372.
36. A. Michalska and K. Maksymiuk, *J Electroanal Chem*, 576 (2005) 339.
37. A. Michalska and K. Maksymiuk, *Anal Chim Acta*, 523 (2004) 97.
38. E. Barsoukov and J.R. Macdonald, *Impedance Spectroscopy Theory, Experiment, and Applications*, second ed. A John Wiley & Sons, Inc., (2005) New Jersey, USA.
39. M. Fibbioli, W.E. Morf, M. Badertscher, N. de Rooij and E. Pretsch, *Electroanalysis*, 12 (2000) 1286.
40. J. Zhu, X. Li, Y. Qin and Y. Zhang, *Sens. Actuators, B*, 148 (2010) 166.
41. C. Luo, X. Zuo, L. Wang, E. Wang, S. Song, J. Wang, J. Wang, C. Fan and Y. Cao, *Nano Lett.*, 8 (2008) 4454.

42. H.E. Kormalı Ertürün, A. Demirel Özel, M.N. Ayanoglu, Ö. Şahin and M. Yılmaz, *Ionics*, 23 (2017) 917.

© 2018 The Authors. Published by ESG (www.electrochemsci.org). This article is an open access article distributed under the terms and conditions of the Creative Commons Attribution license (<http://creativecommons.org/licenses/by/4.0/>).